

Article

Aspects Regarding the Modelling and Optimization of the Transesterification Process through Temperature Control of the Chemical Reactor

Ruxandra-Cristina Stanescu , Cristian-Ioan Leahu  *  and Adrian Soica

Department of Automotive and Transport Engineering, Transilvania University of Brasov,
500036 Brasov, Romania

* Correspondence: leahu.cristian@unitbv.ro

Abstract: Currently, biofuels represent a solution for the European Union in the transportation sector in order to reduce the greenhouse gas (GHG) emissions and the dependency of fossil fuels. Biodiesel from vegetable oils is a solution for countries with low GDP per capita to strengthen the internal agriculture, provide jobs, and reduce the use of fossil fuels. In this study, we model and simulate a temperature regulator designed for the biodiesel transesterification process in a discontinuous batch reactor, using methanol and a homogenous basic catalyst. The simulation was based on the kinetical model of the transesterification reaction and the mathematical model of the reactor. We considered molar ratios of alcohol/oil of 6:1 and 9:1, respectively, to shift the reaction equilibrium towards the production of fatty acid methyl esters. In the design of the simulation, the methanol boiling point was considered a restriction, therefore, temperatures below 65 °C were imposed. The results demonstrate that the increase in temperature results in a decrease in the reaction time and a higher yield, especially for the 6:1 molar ratio reaction, and that the optimum temperature for the batch reactor is of 60 °C. Automatic control improves the performance and costs of production.

Keywords: biofuel; transesterification; reactor; temperature control



Citation: Stanescu, R.-C.; Leahu, C.-I.; Soica, A. Aspects Regarding the Modelling and Optimization of the Transesterification Process through Temperature Control of the Chemical Reactor. *Energies* **2023**, *16*, 2883. <https://doi.org/10.3390/en16062883>

Academic Editor: Mark Laser

Received: 20 February 2023

Revised: 9 March 2023

Accepted: 17 March 2023

Published: 21 March 2023



Copyright: © 2023 by the authors. Licensee MDPI, Basel, Switzerland. This article is an open access article distributed under the terms and conditions of the Creative Commons Attribution (CC BY) license (<https://creativecommons.org/licenses/by/4.0/>).

1. Introduction

At the time being, considering the global socio-economical context, environmental issues and the geopolitical situation in Europe, the European Union, and the rest of the world are looking for alternative ways to secure the energetic sector. The two main goals in the energy sector are now the reduction in greenhouse gas (GHG) emissions and the dependency of fossil fuels. The European Commission published a RePowerEU Communication in March 2022 [1] with the main focus on reducing the dependence on imported fossil fuels. Even though electricity and gas are the dominators in the Communication, EU still relies on imported fossil fuel, therefore, at least biofuels must be taken into consideration [2].

The energy consumption in 2019 in the transport sector accounted for 31% of EU share of energy consumption, being the second biggest consumer after households and services sector. In the transport sector, the highest values are registered in the road transport with a 93% share [3]. As the transport sector represents one of the major contributors to both energy consumption and greenhouse gas (GHG) emissions, there is much focus on this sector to reduce the dependency on fossil fuels. Consumption and emissions in the transport sector are directly related to demographics and economy [4].

According to [3], in 2019, the transport sector accounted 25.8% of total GHG emissions, equivalent to 967.5 million tons CO₂, showing an increase of 3.8% in the last 10 years. The road transport makes up a total of 792.8 million tons CO₂ equivalent, representing 71.7% of total transport emissions. GHG emissions from passenger cars represented 43.4% of the total transport sector emissions, a quite stable position in the last 10 years. Light-duty vehicles added an extra 87.5%, meaning a total of 7.9 million tons equivalent CO₂.

We have to take into consideration that population in the EU is increasing by 0.2% in 2019/2020. The passenger car stock has increased to 247.4 million units in 2019 in EU-27 with a total of 4325 billion pkm. Additionally, the car transport increased as well by 18.2% in the 2000–2019 time frame.

The average age for passenger cars in EU is 11.8 years, Romania presenting the highest value of 16.9 years of use for a passenger car. There was an increase in the number of cars in the EU to 560 units/1000 inhabitants, demonstrating a rise in the last five years. The share of passenger cars by fuel type existing in 2020 in the EU are the following: diesel 51.7%; gasoline 42.8%; and battery electric, plug-in hybrid, and hybrid electric altogether make up 2.3% [5]. However, the new sales of passenger cars by fuel type in the same year show different figures—diesel 28%, gasoline 47.5%, Electrically chargeable (ECVs) 10.5%, Hybrid electric 11.9%, and others (NG, LPG + E85, Fuel cell) 2.1%. Overall, conventional fueled cars made up for 75.5% of cars sales in EU in 2020—a decrease in sales for diesel engines and a substantial increase for the ECVs (doubled) and hybrid electric cars (tripled sales).

The market for ECVs is rapidly rising but mostly in those countries with a high GDP per capita. Affordability is still a barrier to consumers and infrastructure represents a blockage as well.

Biofuels represent a high potential replacement source for fossil fuels in the transport sector, even more so because biofuels can contribute to a reduction in pollutant emissions generated from internal combustion engines [6,7]. For countries with low GDP per capita, biofuels are and will be further a solution to strengthen the internal agriculture, provide jobs, and reduce the use of fossil fuels [2,8]. There has been a constant debate of food over fuel, concerning the use of food-crops lands for biofuel production. However, the data show that biodiesel production reduced Europe's protein imports for animal feed because the processing of oilseeds for biodiesel produced 60% of animal feed and 40% vegetable oils [2,8]. The bioethanol production process creates high protein animal feed, aside from the GHG saving and captured CO₂ [8]. Renewable ethanol capacity of reducing the GHG emissions increased each year to a current level of 76.9% on average compared to fossil fuels in 2021 [9,10].

Biomass represents the feedstock for biofuel production; therefore, the combustion of these biofuels principally is considered to be CO₂ neutral (this applies only for direct emissions from biofuel combustion). The emissions during the full life cycle of biofuels, from changes in land use to combustion of fuels, determine their impact on the climate [8]. According to the European Parliament press release on July 2022, the decarbonization of EU will continue by allowing the Member States to follow up their plans for crop-based biofuel production for transport energy mix [10].

The term “biofuel” refers to “liquid fuel for transport produced from biomass” according to Directive 2018/2011/EC. The most promising biofuels from biomass are biodiesel, bio-ethanol, pure vegetable oil, and bio-methane, along with second-generation biofuels such as bio-hydrogen and Biomass-to-Liquid fuels. The share of biofuels in diesel and gasoline fuels for transport increased from 7.4% to 8.1% for biodiesel and from 6.1% to 6.8% for bioethanol from 2019 to 2020 [11]. The share of bio-components in the transport fuels varies for each country in the EU. In the transport sector, biodiesel represents the largest source of renewable fuel with a total consumption of 12,949 ktoe in 2019 [3], of that 80% of the feedstock is made up from vegetable oils such as rapeseed, soybean, and palm oil, mainly produced through Fatty Acid Methyl Ester (FAME) transesterification or hydrotreatment of vegetable oils. Bioethanol consumption was 2705.7 ktoe, according to Eurostat figures [3]. Production capacity figures are approximately the same, for both biodiesel and bioethanol.

The raw material used for biofuel production is diverse, thus the biofuels characteristics and the physical-chemical properties vary accordingly. These parameters also depend on the production technology.

This paper analyzes the parameters that influence the biofuel production process. Biodiesel production technology is based on the transesterification reaction as its main

process. Usually, in a chemical process, such as the transesterification process discussed here, the basic sequence involves a chemical reaction followed by a separation. Thus, in a reactor, the feedstock and the catalyst are mixed together so that one or more chemical reactions can occur. The reactor design must consider maximizing the conversion rate of the raw material into desired products (high reaction rate and yield) and reducing the reaction time for costs efficiency (increased reaction speed). For the modelling and design of chemical reactors, it is of utmost importance to control and monitor the parameters that influence the transesterification process. Controlling the reaction parameters generates a good reaction yield, an optimum conversion rate, and, finally, a fuel with properties similar to those of conventional diesel fuel. The modelling and simulation of the reaction are described in the paper as a necessity for a better observation of the influence of some parameters on the transesterification reaction. As a result, the molar ratio and reaction temperature are two of the most important parameters for the reaction's progress. This phase is essential for designing a transesterification reactor.

The regulation of temperature presents complex aspects compared to other possible regulations (pressure, volume, flow) because the heat transfer involves complex phenomena associated with high time constants. Temperature regulation represents a stabilization regulation, which actually implies heat-transfer-related problems, regardless of the way the transfer is performed (radiation, conduction, or convection). The heat exchange between the reactor jacket, where the thermal agent flows, and the fluid in the reactor is possible considering a relatively high time constant. Moreover, the temperature transducers are characterized by thermal inertia, therefore, they must be positioned in an area where the heat transfer is at a maximum [12]. Thus, this paper presents the effects of a temperature regulator for a transesterification reactor in order to maintain the temperature at an optimum value.

The remainder of this paper is organized as follows: the aspects of biodiesel production and the transesterification reaction is presented in Section 2. Then, the temperature regulation for a discontinuous chemical reactor operation is presented in Section 3, where an automatic temperature control system is designed and simulated. Section 4 contains discussions and, finally, the conclusion is described in the last section.

2. Aspects of Biodiesel Production

2.1. Feedstock

With the exception of the direct combustion of wood and straws, raw biomass cannot be used directly into reactors to produce energy or fuels. Depending on the physical state and nature of the feedstock and the water content that directly influences the calorific power, there are three main ways for biomass conversion into biofuels: thermo-chemical, bio-chemical, and thermo-mechanical processes.

Depending on the feedstock type, biofuels are divided into four main categories: first, second, and third generation biofuels [13,14]. First generation biodiesel is produced from vegetable oils coming from edible crops such as rapeseed, soybean, sunflower, palm oil, coconut, peanut, etc. Second generation feedstock for biodiesel production includes animal fats, used cooking oils, and non-edible crops such as pine oil, tall oil, castor oil, etc. Third generation biodiesel is produced from algae [15–17]. Fourth generation biodiesel aims to convert solar energy directly into fuel from raw material [13].

The properties of pure vegetable oils make them unsuitable for direct use for compression ignition engines, but these properties can be improved by breaking the triglyceride molecules into lighter ones with the aid of methanol or ethanol through the transesterification process [18].

Biodiesel from vegetable oils is produced through transesterification by converting the glycerides present in the feedstock into products with similar properties with conventional diesel. The raw materials are mainly made of tryacylglycerols, or TAG, and are often named glycerides [19]. Chemically, tryacylglycerols are esters of fatty acids with glycerol (1,2,3-propanetriol; glycerol is often called glycerin) [18,20]. Triglycerides are hydrophobic, water-

insoluble substances, consisting of three moles of fatty acids and one mole of glycerol [21]. Fatty acids are aliphatic, usually straight chain, monocarboxylic acids.

The major reason that vegetable oils and animal fats are transesterified to alkylesters (biodiesel) is that the kinematic viscosity of the biodiesel is much closer to that of petrodiesel. The high viscosity of untransesterified oils and fats leads to operational problems in the diesel engine such as deposits on various engine parts.

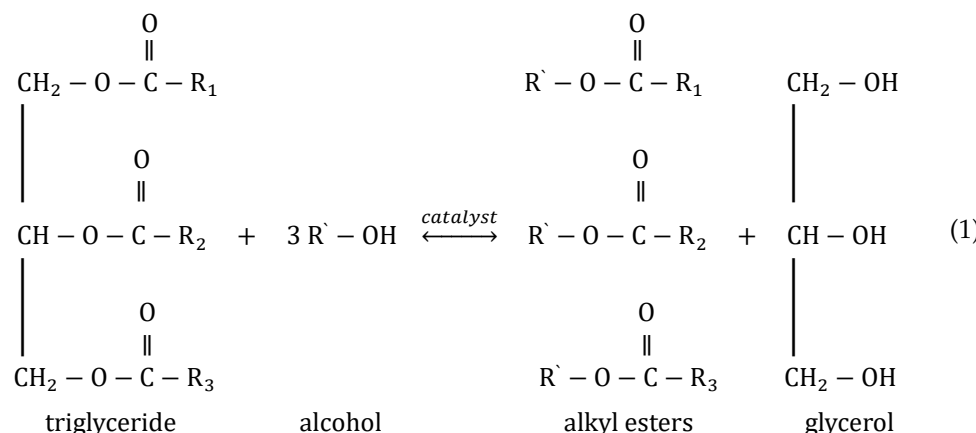
The biodiesel properties, such as ignition qualities, clogging point, cold flow, cetane number, boiling point, oxidation stability, viscosity, and lubricity, depend on the structure of the fatty acids found in the fuel.

2.2. The Transesterification Reaction

The transesterification reaction is used to reduce the viscosity of vegetable oils and animal fats so that the resulting fuel—biodiesel—could be used in internal combustion engines [18]. Transesterification, also called alcoholysis, is the chemical reaction where the oil is mixed with an alcohol in the presence of a catalyst to obtain biodiesel.

The transesterification reaction is: slow—the product is obtained in a time-frame that depends on the feedstock and the alcohol used in the reaction; limited—the reaction is reversible and, therefore, limited. To increase the yield, more alcohol must be added, and this results in a change in the reaction balance; and athermal—the esterification reaction does not need energy for it to occur, but the reaction speed and yield would increase in the presence of a certain temperature. Additionally, the reaction is not exothermic.

Triglycerides (long chain esters of glycerin—alcohol with a hydroxyl group attached to each of the three carbon atoms) in reaction with alcohol produces fatty acid alkyl esters and glycerin. The chemical reaction of transesterification is presented in Equation (1).



The transesterification reaction mechanism was first formulated by Ekey [22]. It consists of a process in three steps: first, the triglycerides transform into diglycerides and then into monoglycerides. All three reactions are reversible, but the reaction balance goes in the direction of forming esters and glycerin [23].

2.3. Factors Influencing the Transesterification Reaction

Analysis of the parameters that influence transesterification is necessary because controlling of these parameters determines an optimum conversion and reaction yield and, thus, appropriate properties for the resulting fuel.

2.3.1. Free Fatty Acids (FFA) and Water Content in the Feedstock

Biodiesel feedstock fits into three categories [24]:

- Refined oils with a FFA content of less than 1.5%;
- Animal fats and yellow oils—FFA < 4%;
- Animal fats with high FFA content $\geq 20\%$.

For a basic catalysis, the FFA should be <3%. The higher the oil acid content, the lower the conversion rate and the yield [25]. Too much or too less alcohol in the reaction may lead to soap formation [26]. Water content influences the conversion rate in the same way. Soap presence in the final product causes high viscosity, gel formation, and leads to a complex glycerin separation process [27].

2.3.2. Catalyst

The catalyst in the transesterification reaction allows a faster reach of the balance state, without interfering with the reaction balance. Depending on the feedstock properties (water content and fatty acids composition), the biodiesel will be produced by transesterification through homogenous, heterogenous, or enzymatic catalysis. The catalysts may be basic or acid, each with their own pros and cons (Table 1).

Table 1. Different types of catalysts used in the transesterification reaction for biodiesel production and their advantages and disadvantages [13,28–30].

Types of Catalysis	Catalysts	Advantages	Disadvantages
Homogenous	Basic: KOH, NaOH, NaOCH ₃ , etc.	<ul style="list-style-type: none"> soluble in the reaction medium; temperature range in batch reactor 25–85 °C at atmospheric pressure; suitable for small size/low cost equipment; catalysts are accessible and have low costs; the catalyst is lost after the reaction through washing and neutralization; glycerin neutralization costs are low. 	<ul style="list-style-type: none"> soap formation function of FFA profile; catalyst/product separation is difficult (involves washing and neutralization); glycerin purification process is complex.
	Acid: H ₂ (SO) ₄ , HCl, etc.	<ul style="list-style-type: none"> the possibility of simultaneous esterification of FFAs and transesterification of triglycerides. 	<ul style="list-style-type: none"> high reaction temperature; high alcohol-to-oil ratio; increased duration of the process; equipment erosion due to substance contact.
Heterogenous	Basic: CaO, MgO, SrO, etc.	<ul style="list-style-type: none"> catalyst recovery and reuse after the reaction occurs (through centrifugation and filtration); low-cost synthesis of catalysts; environmental safety. 	<ul style="list-style-type: none"> slow reaction rate; high reaction temperature (180–200 °C); high pressure (40–60 bar); byproduct formation; sensitivity to free fatty acids.
	Acid: ZrO ₂ , SnO ₂ , TiO ₂ , zeolites, sulfonic ion-exchange resins, etc.	<ul style="list-style-type: none"> catalyst recovery and reuse after the reaction occurs; low toxicity; lower corrosion attack than a homogeneous acid catalyst. 	<ul style="list-style-type: none"> low activity; high duration of the process; high cost of catalysts; undesirable side reactions.
Enzymes: bacterial, fungal and yeast lipases		<ul style="list-style-type: none"> moderate reaction temperature (30–50 °C); low alcohol-to-oil ratio; simple enzyme separation; no need to recover unreacted; methanol and wastewater treatment; enzymes are biodegradable; no formation of by-products. 	<ul style="list-style-type: none"> low reaction rate (compared to alkali catalyzed transesterification); high enzyme production costs; alcohol inhibits the enzymes; gradual deactivation; limited to no regeneration of enzymes.

For oils with a low content of FFA, usually, a basic catalyst is used in a homogenous environment, this being the most cost-effective technology, with low temperature and pressure needed. Heterogenous catalysis, more often used for converting waste-oils to biodiesel [30], has more severe conditions for pressure and temperature [31,32]. Nevertheless, recent advances in technology mention higher yields and purity of the final product and lower energy consumption [33]. Enzymatic catalysis has a long reaction time, but microwave heating allows for shorter reaction time.

Alkali catalyst reaction has a high conversion rate of triglycerides into methyl esters with a short enough reaction time, but it is energy consuming, glycerin recovery is difficult, and the catalyst must be removed from the final product through washing and neutralization [26].

2.3.3. Reaction Temperature

Even though the transesterification reaction can occur without the use of energy, the reaction time and conversion rate are directly influenced by the temperature at which the reaction takes place. An optimum temperature can lead to a decrease in oil viscosity, shortening the reaction time and increasing the reaction speed [34].

Because there is an alcohol involved in the reaction, the temperature must not exceed the alcohol boiling point so it will not vaporize. Additionally, a temperature too high will lead to a decrease in the conversion rate due to soap formation [23,35].

2.3.4. Molar Ratio—Alcohol/Oil

A variable that greatly influences the methyl esters yield is the alcohol-triglycerides molar ratio. For the transesterification reaction, the stoichiometric ratio needs three mols of alcohol to one mol of triglycerides, resulting three mols of fatty acids alkyl esters and one mol of glycerin. The molar ratio is associated with the type of catalyst used for the reaction. According to [36], a molar ration of 6:1 should be used for an optimum conversion for alkali catalysis.

2.4. Transesterification Reaction Kinetics

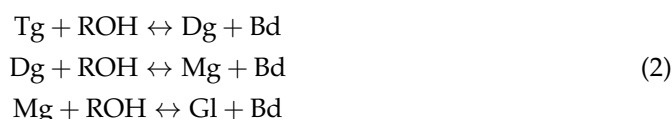
In the case of designing the transesterification chemical process as part of the biodiesel production plant, the experimental approach can be costly, both in time and money invested. The theoretical approach offers the mathematical modeling and simulation of the process, which reduces the time considered for the experiments. Furthermore, it can predict appropriate values for the process design, which can be experimentally verified afterwards.

Mathematical modeling of the reversible chemical reactions that take place during the transesterification process is a must before designing a biodiesel reactor.

The study of the transesterification reaction kinetics offers valuable information on the parameters that can predict the reaction behavior and pattern at any given moment in specific conditions.

Kinetic studies of transesterification are rare, but the mechanisms suggested so far converge and adapt better to the experiments. Freedman [27] published results of the kinetic studies of the transesterification reaction first, followed by Noureddini [37].

Freedman [27] suggested a model based on a three-step reaction, as shown in Equation (2):



where Tg is triglyceride, and Mg and Dg are the mono and diglycerides. Gl is glycerol. ROH and Bd denote the alcohol and ester concentrations.

These reactions are of a secondary order in total in both directions, but the direct reactions are of a pseudo-first order if the molar ratio of alcohol-triglyceride is too high.

Noureddini [37] also considers the transesterification reaction in three stages with each intermediate reaction as a second-order reaction. The total reaction is shown in Equation (3):



where $k_1 - k_8$ are the reaction speed constants.

The Noureddini [37] model is satisfying, considering the correlations with experimental data, but it does not take into consideration the parallel reactions that take place in the reaction environment, such as saponification and the water content effect. However, this model considers the stirring intensity and the effect of temperature on the conversion rate. It also gives values for the activation energy for the transesterification simulation at different temperatures and stirring rates.

The Komers [38] model takes into consideration for the modelling of the reaction, the saponification, and the water content effect, being the most complex model found in the literature. The Komers [38] model is shown in Equation (4):



where Uv is the oil used in the reaction.

The reaction mechanism of the phenomena that interferes in the reaction tank was described by Komers in [38]. The main difficulty in this model is the high number of speed reaction's constants (18 in total).

Each reaction is reversible with the different speed reaction constant k_i , thus observing that the direct and indirect reactions occur at a different speed.

3. Temperature Regulation for Discontinuous Tank Operation

Is worth taking into consideration that the most important parameters that describe the chemical process are mass, energy, and momentum, and these are characterized by density, volume, temperature, pressure, flow, etc., when they cannot be measured directly. Some input parameters influence the reaction directly; thus, we considered it vital to model and simulate the reaction beforehand, confirming that the molar ratio and temperature were very important parameters in designing the process.

A system and its behavior are characterized by two things:

- A fundamental set of parameters with values that describe the system's natural state;
- A set of equations with aforementioned variables that describe how the system's natural state modifies with time.

3.1. Mathematical Model

In order to design a temperature regulation for a chemical reactor, first, the mathematical model for a convection heat transfer process has to be determined, where the thermal agent warms up a product in liquid phase.

For a given reaction, it is similar with the transesterification Reaction (5):



The surfactants were loaded in the reaction tank and steam was introduced in the tank shell to bring the mixture to the required temperature. Then, cooling water was added to help reduce the temperature, if needed, and for the reactor to follow the desired temperature profile as a function of time. The temperature profile was loaded in the temperature controller as a start signal.

If the reaction was stopped too early, then the A and B components would not react enough (total); thus, the conversion rate and yield were low. There is an optimum duration for the reaction. In addition, there was an optimum temperature profile for the reactor tank

to follow. Considering the strict relation between reaction speed constants and temperature, the reaction should take place at the maximum temperature possible in order to reduce to a minimum the time spent in the tank. This maximal temperature was a limit imposed by several constraints as maximum work temperature, pressure in the tank, and product and/or surfactants degrading at high temperatures.

Due to the tank characteristics (discontinuous), there was no input or output flow, and all of the components were introduced in the tank at the beginning and extracted when the reaction was completed.

We assume the density (ρ) and volume (V) in the chemical reactor are constant. Thus, the continuity equation for the reaction mass or the total mass balance at the beginning of the reaction is:

$$\frac{d(\rho V)}{dt} = 0 \quad (6)$$

The continuity equation for component A is given in Equation (7):

$$V \frac{dc_A}{dt} = -Vkc_Ac_B \quad (7)$$

For component B:

$$V \frac{dc_B}{dt} = -Vkc_Ac_B \quad (8)$$

Energy balance for the process is presented in Equation (9):

$$\rho V C_p \frac{dT}{dt} = -\lambda V c_A c_B k - h_i A_i (T - T_M) \quad (9)$$

The temperature in the reaction tank has to fulfill an optimization criterion such as:

- Optimum constant operation temperature;
- The best temperature profile function of time in the tank.

3.2. Temperature Control Design

The maximum temperature results from the components thermal stability, tank design and material, and from the catalyst's properties (Figure 1).

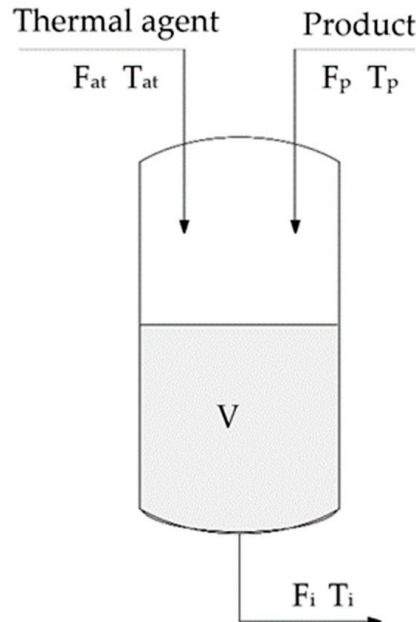


Figure 1. Schematic of a process with temperature control.

The following notations are used in the figure: F_{at} —thermal agent flow; T_{at} —thermal agent temperature; F_p —product flow; T_p —product temperature; F_i —output product flow; and T_i —output product temperature.

The control of temperature involves complex phenomena with increased time constants, therefore, temperature control is a stabilization control, meaning heat-transfer-related problems, regardless of the way the heat transfer is performed.

Considering a dynamic regimen, the accumulated heat is represented by the difference between the input and the output of the caloric flow, as seen in Equation (10):

$$\rho_{at}F_{at}(t)c_{at}T_{at} + \rho_pF_p(t)c_pT_p = \rho_iF_{i0}c_iT_i(t) + \rho_iVc_i\frac{d}{dt}T_i(t) \quad (10)$$

and

$$F_{at}(t) + F_p = F_i(t) \quad (11)$$

If we consider $u(t) = \frac{\Delta F_{at}(t)}{F_{a0}}$ the input value and $y(t) = \frac{\Delta T_i(t)}{T_{i0}}$ the regulated output value, we receive:

$$\frac{V}{F_{i0}}\frac{d}{dt}y(t) + y(t) = \frac{\rho_{at}c_{at}T_{at} - \rho_i c_i T_{i0}}{\rho_i c_i T_{i0}} \frac{F_{a0}}{F_{i0}} u(t) \quad (12)$$

thus, the transfer function:

$$G_p(s) = \frac{k_p}{T_p s + 1} \quad (13)$$

where $T_p = \frac{V}{F_{i0}}$ represents the time constant and $k_p = \frac{\rho_{at}c_{at}T_{at} - \rho_i c_i T_{i0}}{\rho_i c_i T_{i0}} \frac{F_{a0}}{F_{i0}}$ is the amplifying factor.

To design a system with automated temperature regulation, we have to consider the transfer function for the static part as follows:

$$G_f(s) = \frac{k_T}{T_T s + 1} \cdot \frac{k_E}{T_E s + 1} \cdot \frac{k_p}{T_p s + 1} = \frac{k_f}{(T_T s + 1)(T_E s + 1)(T_p s + 1)} \quad (14)$$

where, all connected in series, the index represents T—the temperature transducer; E—the execution element; and p—the process.

We cannot neglect the delay constant, which is high for the thermal transfer process, significant for temperature transducer, and lower for the execution element. Therefore, the regulation algorithm should take into consideration an anticipatory effect.

A second-degree closed system is represented by Equation (15):

$$G_0(s) = \frac{\omega_n^2}{s^2 + 2\zeta \cdot \omega_n s + \omega_n^2} \quad (15)$$

and the transfer function for the open circuit is:

$$G_d(s) = \frac{\frac{\omega_n^2}{2\zeta}}{s\left(\frac{1}{2\zeta \cdot \omega_n} s + 1\right)} \quad (16)$$

where ω_n (natural pulsation) and ζ (damping factor) give the dynamic performances of the system.

We consider the process for the transesterification reaction: vegetable oil reacts with methanol in the presence of a catalyst to produce fatty acid methyl esters (FAME) and glycerin. This process should consider the following constraint: the temperature should remain the same for the duration of the reaction so that the reaction balance goes in the right direction—formation of FAME, with a defined time frame and with minimum formation of coproducts (soaps, etc.). For this system (Figure 2), we have determined the:

- Mathematical model of the system based on balance equations;
- The transfer functions;
- Regulators type and parameters.

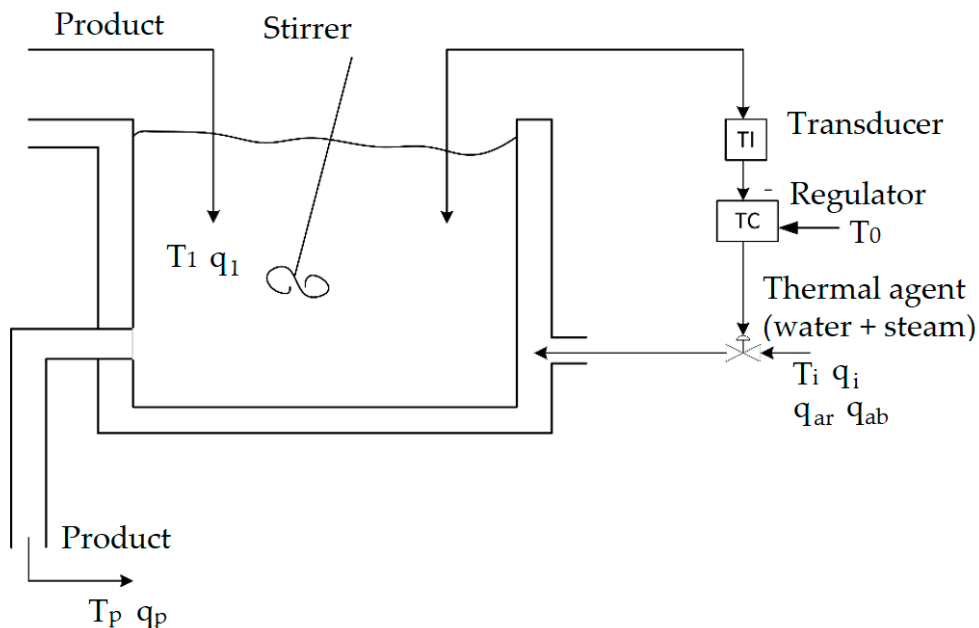


Figure 2. Schematic of the temperature control system.

The following notations are used in the figure: T_1 —temperature of the product inside the reactor; q_1 —heat of the product in the reactor; T_0 —reference temperature; T_i —thermal agent temperature; q_i —thermal agent heat; q_{ar} —cold water heat; q_{ab} —steam heat; T_p —final product temperature; and q_p —final product heat.

Because the reaction is endothermic, we have considered only the energy balance as follows in the mathematical model:

Heat balance equations are:

$$q_{ar} + q_{ab} = q_p \quad (17)$$

and

$$F_{ar}c_{ar}T_{ar} + F_{ab}h_{ab} = C_p \frac{dT_p}{dt} + F_p c_p T_p \quad (18)$$

where F_{ar}, c_{ar}, T_{ar} represent heat from cold water; F_{ab}, h_{ab} —heat from steam; $C_p \frac{dT_p}{dt}$ —time constant for the product's temperature; and F_p, c_p, T_p —heat transferred through the final product.

For this system we considered designing a Proportional Integral (PI) regulator, which had a zero stationary error and a maximum 5% overclocking. The transfer function for the PI regulator is:

$$G_f(s) = G_E(s) \cdot G_p(s) \cdot G_T(s) \quad (19)$$

and the transfer function for the open loop system is:

$$G_d(s) = G_R(s)G_f(s) = k_R \frac{T_i s + 1}{T_i s} \cdot \frac{k_f}{(T_E s + 1)(T_p s + 1)} \quad (20)$$

To determine the parameters for the regulator we considered $T_i = T_p$.

Both Equations (19) and (20) are second-degree functions; thus, we can identify the parameters and coefficients of the regulator, as shown in the equation:

$$G_d(s) = \frac{k_R \cdot k_f}{T_i s (T_E s + 1)} = \frac{\frac{\omega_n}{2\zeta}}{s \left(\frac{1}{2\zeta\omega_n} s + 1 \right)} \quad (21)$$

3.3. Simulation

According to the existing literature [12,39–42], we consider the transfer function for the execution element:

$$G_E(s) = \frac{k_E}{T_E s + 1} = \frac{2}{360s + 1} \quad (22)$$

and for the transducer:

$$G_T(s) = 2 \quad (23)$$

The mathematical model of the process is described best by a differential equation, with T_p being the time constant as follows:

$$T_p = \frac{M_p}{F_p} = \frac{400}{21} \simeq 19\text{min} = 1143\text{ s} \quad (24)$$

For the temperature regulation loop, we consider the process transfer function in equation:

$$G_p(s) = \frac{k_p}{T_p s + 1} \quad (25)$$

with $k_p = 1$.

From Equations (22)–(24), the transfer function for the components is represented by Equation (26):

$$G_f(s) = G_E(s) \cdot G_p(s) \cdot G_T(s) = \frac{2}{360s + 1} \cdot \frac{1}{1143s + 1} \cdot 2 = \frac{4}{(360s + 1)(1143s + 1)} \quad (26)$$

We also considered the overclocking of 4.3% (<5%), resulting in the dumping factor $\zeta = 0.7$, following:

$$k_R = \frac{\omega_n T_i}{2\zeta k_f} = \frac{0.0019 \cdot 1143}{2 \cdot 0.7 \cdot 4} = 0.38 \quad (27)$$

$$\omega_n = \frac{1}{2\zeta T_E} = 0.0019 \quad (28)$$

and the transfer function:

$$G_R(s) = \frac{0.38 \cdot 1143s + 0.38}{1143s} \quad (29)$$

Simulation for the temperature regulation of the transesterification process, based on the energy balance, was performed in MATLAB Simulink following the regulation setup from Figure 3.

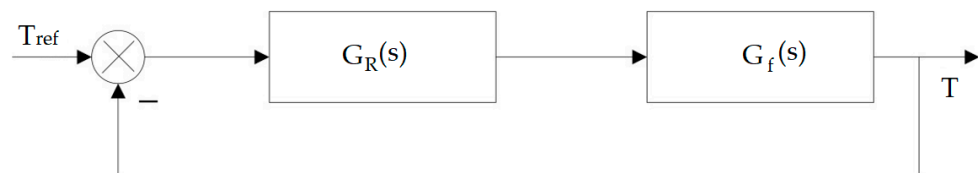


Figure 3. Temperature regulation setup in MATLAB Simulink.

The MATLAB simulation resulted in the temperature profile, shown in Figure 4, for a maximum reference temperature of 60 °C.

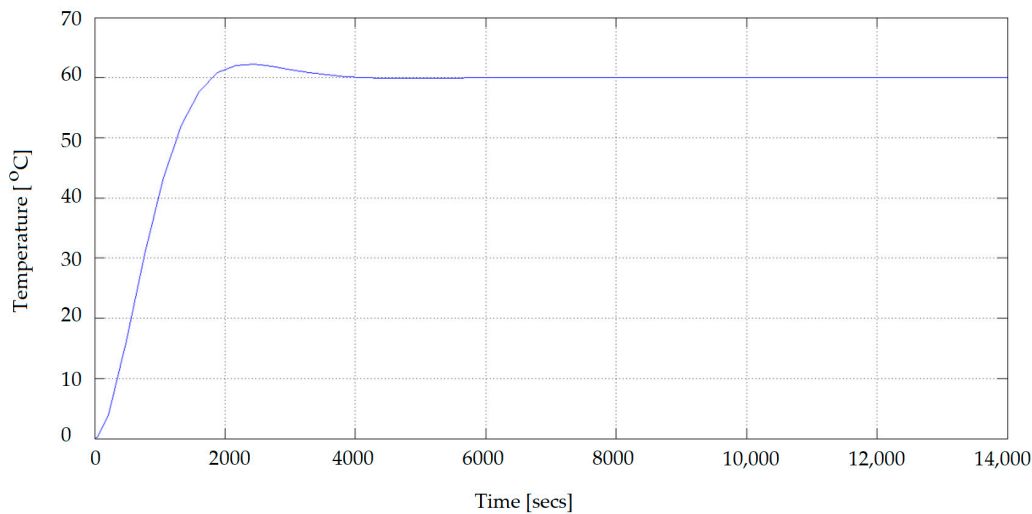


Figure 4. Temperature profile curve.

Based on the simulation, we identified the following performances of the automatic temperature control system:

$$e_{st} = 0; \sigma = 3.75\%; t_s = 3008s \quad (30)$$

where e_{st} represents stationary error; σ —overclocking; t_s —stabilizing time, which demonstrates that by following the constraints imposed for obtaining the desired performances, and the regulator was designed correctly. The parameters used in the simulation were chosen based on the existing literature [12,39–41,43] and from repeated simulations in order to obtain a negligible stationary error and an overclock <5%, which was attained. As the boiling point of methanol is 64.8 °C, the temperature in the reactor should not exceed this value; therefore, the temperature was set at 60 °C.

3.4. Mathematical Approach—Validation of the Simulation Results

For the mathematical modelling of the transesterification reaction, we considered the speed constants $k_1 \dots k_6$ and the activation energy values $E_1 \dots E_6$ from [37] on soy oil using an alkali catalyst, and the results are given in Table 2.

Table 2. Rate constant and activation energy values [37].

Rate Constant	Value	Activation Energy	Value
k_1	0.050	E_1	13,145
k_2	0.110	E_2	9932
k_3	0.215	E_3	19,860
k_4	1.228	E_4	14,639
k_5	0.242	E_5	6421
k_6	0.007	E_6	9588

The values of the speed constants can be predicted based on the activation energy values at different temperatures, using the Arrhenius equation:

$$k = k_0 \exp\left(-\frac{E}{RT}\right) \quad (31)$$

where R —gas constant; T —absolute temperature; E —activation energy; k_0 —preexponential factor; and index 0 suggests that the products and surfactants are considered in standard conditions [43–45].

From Equation (31), it can be noted that speed can be a function that increases (exponentially) with temperature and depends on the magnitude of the activation energy E .

For the simulations in this work, we considered the transesterification reaction of soybean oil with methanol, using a basic catalyst in a homogenous catalysis. The parameters for equation (31) were calculated from the experimental data gathered from [37,38,46–49]. Usually, homogenous catalysis is used a constant temperature from around 50 to 60 °C at atmospheric pressure [20]. From the analysis of the reaction at different constant temperatures (50, 55, 60, and 65 °C), and from the experimental values given in [37,38,46–49], it can be noted that the methyl esters yield drops at temperatures higher than 60 °C (Figures 5 and 6).

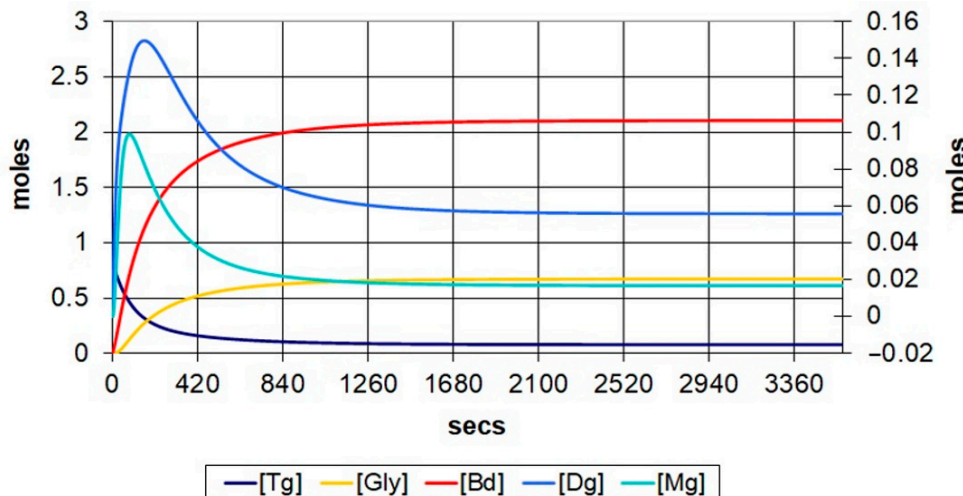


Figure 5. Transesterification reaction at 60 °C and 6:1 molar ratio.

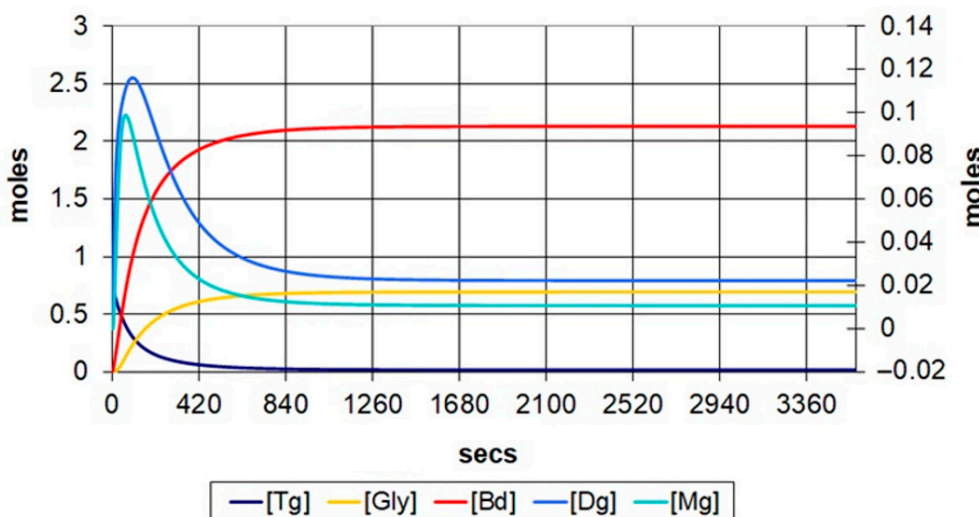


Figure 6. Transesterification reaction at 60 °C and 9:1 molar ratio.

Figures 5 and 6 represent the transesterification evolution at temperature of 60 °C, with molar ratios of 6:1 and 9:1, respectively. It can be observed that the number of mols of methyl esters increases from 2.10 mols to 2.13 mols along with the increase in the molar ratio. The conversion rate increases from 85.27% to 94.91%, and the duration in which the reaction reaches an equilibrium state decreases from 1100 s to 900 s, approximately.

The analysis of methyl esters evolution at different temperatures with 6:1 and 9:1, respective, molar ratios, it can be observed that the conversion rate increases with the increase in temperature, and the stabilizing time decreases by almost half for 6:1 molar ratio and by ~300 s for 9:1 molar ratio, which suggests that the temperature has a higher influence on the reaction time and yield at a 6:1 molar ratio.

In Figure 7, presented is the evolution of methyl esters at different temperatures (50, 55, 60, and 65 °C).

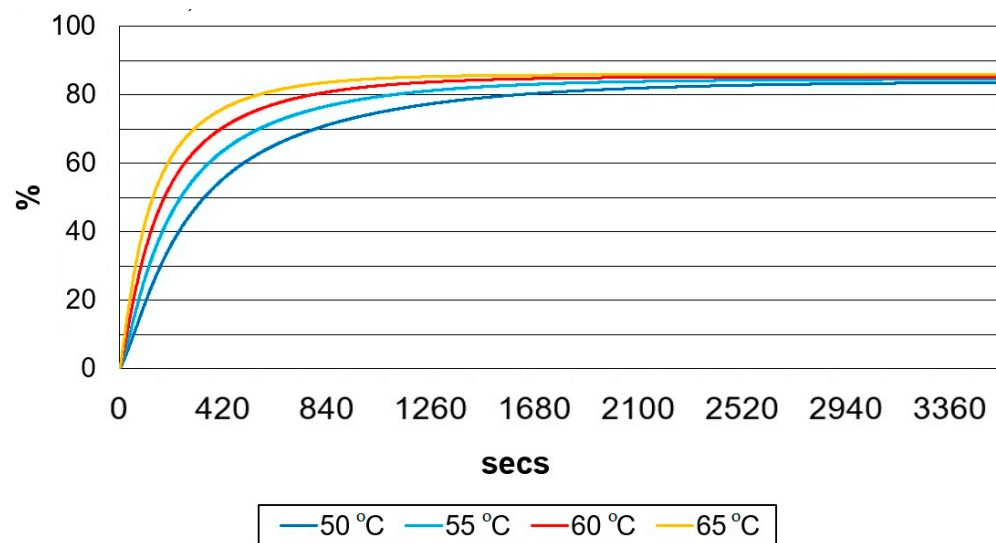


Figure 7. Conversion of methyl esters at different temperatures and 6:1 molar ratio.

In Figure 7, it can be observed that the mass of methyl esters also increases with the increase in temperature. The reaction time also modifies (shortens) with the increase in temperatures. As the temperature in the reactor increases, the viscosity of the oil will decrease, thus the reaction time will be shorter and the reaction rate higher. Even though the simulations were performed at 65 °C, they should not exceed the methanol boiling point (64.8 °C), as the methanol will start to evaporate, and the reaction rate will decrease. This limitation of reaction temperature was considered when we modelled and simulated the temperature regulator.

4. Discussion

In this study, we aimed to model and simulate the behavior of a transesterification batch reactor by controlling the reaction temperature. The transesterification reaction took place in the presence of a catalyst, which allows, without interfering with the reaction equilibrium, a rapid reach of an equilibrium state.

For the homogenous catalysis, the most efficient catalysts have proven to be KOH, NaOH, or NaOCH₃ [13,28]. Among their advantages, we could highlight the high reaction speed, reaction temperature in the range of 25–85 °C, atmospheric pressure, equipment cost, and operation as relatively low. The downside of this type of reaction was the catalyst separation from the final product, which was performed through washing and neutralization, but the costs for the glycerin purification were relatively low. Basic homogenous catalysts were preferred due to the reaction conditions, which were suited for laboratory use or small-scale production units.

The mathematical model for the convection heat transfer process was determined, where the thermal agent heated the product in liquid phase in a tank. The transesterification process requires a constant temperature profile for the reaction to take place with maximum conversion rate and yield. For this condition to be fulfilled, we designed and simulated an automatic temperature control system for a discontinuous tank. For the modelling and simulation, we considered the reaction molar ratios of 6:1 and 9:1, respectively, to shift the reaction equilibrium towards the production of fatty acid methyl esters. The saponification was neglected. For the modelling and simulation of the reaction we considered a fatty acid content < 2%.

The validation of the mathematical results was carried out for the transesterification reaction using a homogenous basic catalyst, due to its accessibility, lower cost, and higher reactive capacities compared to acid catalysis. Along with the chemical reaction, the

feedstock properties were very important for a complete reaction to occur in order to obtain a product with characteristics that match the imposed quality standards for diesel/biodiesel fuel—ASTM D6751. The oil-free fatty acid content greatly influences these properties.

The FFA content of soybean oil (~2%) makes it suitable for homogenous catalysis in the existing batch reactor. The methanol was recovered through evaporation, and the catalyst was separated from the end product by washing and then neutralization.

Reaction speed increased with temperature, but, also, the methyl esters yield dropped at temperatures higher than 60 °C, as the methanol started to evaporate at 64.8 °C. For alkali catalysts, the results showed that the reaction took place at an optimum temperature of 60 °C and a molar ratio of 6:1, with a yield of approximately 90%. Recent works in the field confirmed these results [13,28,29].

From an economical perspective, biofuels from pure vegetable oils have the advantage that the composition is pure, which reduces the pre-processing time and costs, and the final product has a superior quality. Animal fats as feedstock also have economic advantages, but the raw material has a high content of saturated fats, which makes the biodiesel obtained from these sources form gels. Used cooking oils present an environmental advantage (which actually depends on the efficiency of local collection of used oils), but the recycled oils contain impurities that must be removed before the biodiesel production can occur, which actually involves supplementary costs for pre-processing. Promising technologies have been developed in this area, as environmental issues arise from the inappropriate disposal of waste-cooking oils and means to convert them to biodiesel become more accessible [50]. Microalgae are a promising feedstock for biodiesel production, but the high content of unsaturated lipids make the final product become less stable, the fatty acids content varies greatly within species, therefore, the biodiesel properties vary accordingly [13], and they are not yet competitive with fossil fuels in terms of costs [17].

The mathematical analysis shows the importance of maintaining the temperature constant for the entire reaction; therefore, it justifies the need for proper temperature regulation and the correct design for the temperature transducer.

5. Conclusions

In this research we demonstrated that the thermal regimen of the chemical reactor is influenced by factors as:

- Chemical properties of the reaction system: chemical balance, the influence of temperature on the thermal effect, and speed constant;
- Physical properties of the system: temperature and latent heat, specific heat, viscosity, and thermal conductivity;
- Catalyst's sensitivity to temperature and deactivation time;
- Mechanical properties, thermal stability, and resistance to corrosion.

The complex reaction kinetics have shown the necessity of mathematical modelling of the process and its advantages over experimental trials, which involve products and time for testing, thus they are less cost-effective. Regardless, simulation data should always be correlated with in experimental tests.

The work presented in this paper shows a correlation of data obtained through simulation and the experimental studies in the field: the molar ratio and temperature are the most important factors to consider for a maximum conversion rate. A 6:1 molar ratio proves to be the appropriate choice for this setup at 60 °C when using methanol in the reaction.

Author Contributions: Conceptualization, R.-C.S. and C.-I.L.; methodology, R.-C.S. and C.-I.L.; software, R.-C.S.; validation, R.-C.S., C.-I.L. and A.S.; formal analysis, C.-I.L.; investigation, R.-C.S.; resources, C.-I.L.; data curation, C.-I.L.; writing—original draft preparation, R.-C.S.; writing—review and editing, R.-C.S. and C.-I.L.; visualization, C.-I.L.; supervision, A.S.; project administration, A.S. All authors have read and agreed to the published version of the manuscript.

Funding: This research received no external funding.

Data Availability Statement: Not applicable.

Conflicts of Interest: The authors declare no conflict of interest.

References

1. European Commission Website, REPowerEU: Joint European Action for More Affordable, Secure and Sustainable Energy. 2022. Available online: https://ec.europa.eu/commission/presscorner/detail/en/IP_22_1511 (accessed on 7 February 2023).
2. European Biodiesel Board Website, European Sustainable Biodiesel Is Key to Reducing Fossil Fuel Imports and Securing Our Food and Feed Supply. 2022. Available online: https://ebb-eu.org/wp-content/uploads/2022/03/EBB-PR-Reaction-to-RePowerEU-Communication_16March2022_FINAL.pdf (accessed on 7 February 2023).
3. European Commission, Directorate-General for Mobility and Transport, EU Transport in Figures: Statistical Pocketbook 2021. Available online: <https://data.europa.eu/doi/10.2832/27610> (accessed on 7 February 2023).
4. Tarulescu, S.; Tarulescu, R.; Soica, A.; Leahu, C.I. Smart Transportation CO₂ Emission Reduction Strategies. *IOP Conf. Ser. Mater. Sci. Eng.* **2021**, *252*, 012051. [[CrossRef](#)]
5. European Automobile Manufacturers' Association—ACEA. 2022. Report: Vehicles in Use, Europe. 2022. Available online: <https://www.acea.auto/files/ACEA-report-vehicles-in-use-europe-2022.pdf> (accessed on 14 January 2023).
6. Puricelli, S.; Cardellini, G.; Casadei, S.; Faedo, D.; Oever, A.E.M.; Grossi, M. A review on biofuels for light-duty vehicles in Europe. *Renew. Sustain. Energy Rev.* **2021**, *137*, 110398. [[CrossRef](#)]
7. Tutak, W.; Jamrozik, A.; Grab-Rogaliński, K. Evaluation of Combustion Stability and Exhaust Emissions of a Stationary Compression Ignition Engine Powered by Diesel/n-Butanol and RME Biodiesel/n-Butanol Blends. *Energies* **2023**, *16*, 1717. [[CrossRef](#)]
8. Rutz, D.; Janssen, R. *Biofuel Technology Handbook*; WIP Renewable Energies: München, Germany, 2007.
9. European Renewable Ethanol—ePURE Website, EU Ethanol Sets New Record for Greenhouse-Gas Reduction, Confirms Importance to Europe's Energy Independence. 2022. Available online: <https://www.epure.org/press-release/eu-ethanol-sets-new-record-for-greenhouse-gas-reduction-confirms-importance-to-europes-energy-independence/> (accessed on 14 January 2023).
10. European Renewable Ethanol—ePURE Website, A Step in the Right Direction on Biofuels Policy, but More Is Needed. 2022. Available online: <https://www.epure.org/press-release/a-step-in-the-right-direction-on-biofuels-policy-but-more-is-needed/> (accessed on 14 January 2023).
11. Transport & Environment Website, 10 Years of EU Fuels Policy Increased EU's Reliance on Unsustainable Biofuels. 2021. Available online: <https://www.transportenvironment.org/wp-content/uploads/2021/07/Biofuels-briefing-072021.pdf> (accessed on 19 December 2022).
12. Dulău, M. The automation of the continuous processes. In *Chemical and Thermal Processes*; “Petru Maior” University Publishing House: Tîrgu-Mureș, Romania, 2004.
13. Pikula, K.; Zakharenko, A.; Stratidakis, A.; Razgonova, M.; Nosyrev, A.; Mezhuev, Y.; Tsatsakis, A.; Golokhvast, K. The advances and limitations in biodiesel production: Feedstocks, oil extraction methods, production, and environmental life cycle assessment. *Green Chem. Lett. Rev.* **2020**, *13*, 275–294. [[CrossRef](#)]
14. Stanescu, R.C.; Chiru, A.; Muntean, B.A.; Săcăreanu, S. Processes for liquid biofuel production from biomass. In Proceedings of the International Congress on Automotive and Transport Engineering—CONAT, Brasov, Romania, 27–29 October 2010.
15. Stanescu, R.C.; Chiru, A.; Muntean, B.A.; Săcăreanu, S. Algae as a Fuel Resource for the Automotive Sector. In *Automobile and the Environment*; Chiru, A., Ed.; Cambridge Scholars Publishing: Newcastle, UK, 2011; pp. 181–194.
16. Hawrot-Paw, M.; Ratomski, P.; Koniuszy, A.; Golimowski, W.; Teleszko, M.; Grygier, A. Fatty Acid Profile of Microalgal Oils as a Criterion for Selection of the Best Feedstock for Biodiesel Production. *Energies* **2021**, *14*, 7334. [[CrossRef](#)]
17. Neag, E.; Stupar, Z.; Maicaneanu, S.A.; Roman, C. Advances in Biodiesel Production from Microalgae. *Energies* **2023**, *16*, 1129. [[CrossRef](#)]
18. Muślewski, Ł.; Markiewicz, M.; Pajak, M.; Kałaczyński, T.; Kolar, D. Analysis of the Use of Fatty Acid Methyl Esters as an Additive to Diesel Fuel for Internal Combustion Engines. *Energies* **2021**, *14*, 7057. [[CrossRef](#)]
19. Agarwal, A.K.; Gupta, J.G.; Dhar, A. Potential and challenges for large-scale application of biodiesel in automotive sector. *Prog. Energy Combust. Sci.* **2017**, *61*, 113–149. [[CrossRef](#)]
20. Knothe, G.; Krahl, J.; Gerpen, J. Biodiesel Production. In *Biodiesel Handbook*; Gerhard, K., Jürgen, K., Jon, V.G., Eds.; AOCS Press: Champaign, IL, USA, 2010; pp. 31–96.
21. Huber, G.W.; Iborra, S.; Corma, A. Synthesis of Transportation Fuels from Biomass: Chemistry, Catalysts, and Engineering. *Chem. Rev.* **2006**, *106*, 4044–4098. [[CrossRef](#)]
22. Eckey, E.W. Process for Treating Fats and Fatty Oils. U.S. Patent US2378005, November 1941.
23. Fangrui, M.; Hanna, M.A. Biodiesel production: A review. *Bioresour. Technol.* **1999**, *70*, 1–15.
24. Gerpen, J.; Shanks, B.; Pruszko, R. Biodiesel production technology. *Renew. Energy Lab. Subcontract. Rep.* **2004**, *87*, 1–110.
25. Meher, L.C.; Vidya Sagar, D.; Naik, S.N. Technical aspects of biodiesel production by transesterification. *Renew. Sustain. Energy Rev.* **2006**, *10*, 248–268. [[CrossRef](#)]
26. Dorado, M.P.; Ballesteros, E.; Almeida, J.A.; de Schellert, C.; Lörlein, H.P.; Krause, R. An alkali-catalyzed transesterification process for high free fatty acid waste oils. *Trans. ASABE* **2002**, *45*, 525–529. [[CrossRef](#)]

27. Freedman, B.; Butterfield, R.O.; Pryde, E.H. Transesterification kinetics of soybean oil. *J. Am. Oil Chem. Soc.* **1986**, *63*, 1375–1380. [\[CrossRef\]](#)

28. Changmai, B.; Vanlalveni, C.; Ingle, A.P.; Bhagat, R.; Rokhum, S.L. Widely used catalysts in biodiesel production: A review. *RSC Adv.* **2020**, *68*, 41625–41679. [\[CrossRef\]](#) [\[PubMed\]](#)

29. Encinar, J.M.; González, J.F.; Martínez, G.; Nogales-Delgado, S. Transesterification of Soybean Oil through Different Homogeneous Catalysts: Kinetic Study. *Catalysts* **2022**, *12*, 146. [\[CrossRef\]](#)

30. Thangaraj, B.; Solomon, P.R.; Muniyandi, B.; Ranganathan, S.; Lin, L. Catalysis in biodiesel production—A review. *Clean Energy* **2018**, *3*, 2–23. [\[CrossRef\]](#)

31. Chandra Kishore, S.; Perumal, S.; Atchudan, R.; Sundramoorthy, A.K.; Alagan, M.; Sangaraju, S.; Lee, Y.R. A Review of Biomass-Derived Heterogeneous Catalysts for Biodiesel Production. *Catalysts* **2022**, *12*, 1501. [\[CrossRef\]](#)

32. Castillo Gómez, J.P.; Álvarez Gutiérrez, P.E.; Adam Medina, M.; López Zapata, B.Y.; Ramírez Guerrero, G.V.; Vela Valdés, L.G. Effects on Biodiesel Production Caused by Feed Oil Changes in a Continuous Stirred-Tank Reactor. *Appl. Sci.* **2020**, *10*, 992. [\[CrossRef\]](#)

33. Biabani, A.; Khoshhal, A.; Aghel, B. Solar heat for biodiesel production in microchannel. *Fuel* **2023**, *333*, 12670. [\[CrossRef\]](#)

34. Leung, D.Y.C.; Wu, X.; Leung, M.K.H. A review on biodiesel production using catalyzed transesterification. *Appl. Energy* **2010**, *87*, 1083–1095. [\[CrossRef\]](#)

35. Leung, D.Y.C.; Guo, Y. Transesterification of neat and used frying oil: Optimization for biodiesel production. *Fuel Process. Technol.* **2006**, *87*, 883–890. [\[CrossRef\]](#)

36. Tomasevic, A.V.; Siler-Marinkovic, S.S. Methanolysis of used frying oil. *Fuel Process. Technol.* **2003**, *81*, 1–6. [\[CrossRef\]](#)

37. Noureddini, H.; Zhu, D. Kinetics of transesterification of soybean oil. *J. Am. Oil Chem. Soc.* **1997**, *74*, 1457–1463. [\[CrossRef\]](#)

38. Komers, K.; Skopal, F.; Stloukal, R.; Machek, J. Kinetics and mechanism of the KOH—Catalyzed methanolysis of rapeseed oil for biodiesel production. *Eur. J. Lipid Sci. Technol.* **2002**, *104*, 728–737. [\[CrossRef\]](#)

39. Agachi, S. *Automation of Chemical Processes*; Science Book House: Cluj-Napoca, Romania, 1994.

40. Dulău, M.; Olteanu, S. *System Modeling and Simulation: Matlab, Simulink, Spice Applications*; “Petru Maior” University Publishing House: Tîrgu-Mureș, Romania, 2011.

41. Tertișco, M.; Popescu, D.; Jora, B.; Russ, I. *Continuous Industrial Automation*; Didactic and Pedagogical Publishing House: Bucharest, Romania, 1991.

42. Smigelschi, O.; Woinaroschy, A. *Process Optimization in the Chemical Industry*; Technical Publishing House: Bucharest, Romania, 1978.

43. Mihail, R.; Muntean, O. *Chemical Reactors*; Didactic and Pedagogical Publishing House: Bucharest, Romania, 1983.

44. Green, D.W.; Southard, M.Z. *Perry’s Chemical Engineers’ Handbook*, 9th ed.; McGraw-Hill Education: New York, NY, USA, 2019.

45. Sinnott, R.; Towler, G. *Chemical Engineering Design—Principles, Practice and Economics of Plant and Process Design*; Butterworth-Heinemann: Oxford, UK, 2021.

46. Burnham, S.C.; Searson, D.P.; Willis, M.J.; Wright, A.R. Inference of chemical reaction networks. *Chem. Eng. Sci.* **2008**, *63*, 862–873. [\[CrossRef\]](#)

47. Darnoko, D.; Cheryan, M. Kinetics of palm oil transesterification in a batch reactor. *J. Am. Oil Chem. Soc.* **2000**, *77*, 1263–1267. [\[CrossRef\]](#)

48. Santacesaria, E.; Tesser, R.; Di Serio, M.; Guida, M.; Gaetano, D.; Garcia Agreda, A. Kinetics and Mass Transfer of Free Fatty Acids Esterification with Methanol in a Tubular Packed Bed Reactor: A Key Pretreatment in Biodiesel Production. *Am. Chem. Soc. Ind. Eng. Chem. Res.* **2007**, *46*, 5113–5121. [\[CrossRef\]](#)

49. Singh, A.K.; Fernando, S.D. Reaction Kinetics of Soybean Oil Transesterification Using Heterogeneous Metal Oxide Catalysts. *Chem. Eng. Technol.* **2007**, *30*, 1716–1720. [\[CrossRef\]](#)

50. Mohadesi, M.; Aghel, B.; Maleki, M.; Ansari, A. Production of biodiesel from waste cooking oil using a homogeneous catalyst: Study of semi-industrial pilot of microreactor. *Renew. Energy* **2019**, *136*, 677–682. [\[CrossRef\]](#)

Disclaimer/Publisher’s Note: The statements, opinions and data contained in all publications are solely those of the individual author(s) and contributor(s) and not of MDPI and/or the editor(s). MDPI and/or the editor(s) disclaim responsibility for any injury to people or property resulting from any ideas, methods, instructions or products referred to in the content.